Hindawi
International Journal of Aerospace Engineering
Volume 2023, Article ID 4448592, 17 pages
https://doi.org/10.1155/2023/4448592

Research Article

Design and Parameter Optimization of Trajectory Correction Control Strategy for Air Duct Structure Projectile

Silin Cui,[1] **Xing Liu**,[2] **Shoushan Jiang**,[1] **and Wei Wu**[2]

[1]*School of Mechanical Engineering, Northwestern Polytechnical University, Xi'an 710072, China*
[2]*School of Electronic Information Engineering, Xi'an Technological University, Xi'an 710021, China*

Correspondence should be addressed to Xing Liu; linshiyin217@sina.com

Received 17 November 2022; Revised 14 March 2023; Accepted 16 March 2023; Published 13 April 2023

Academic Editor: Qingfei Fu

In order to make the new air duct structure trajectory correction projectile have good dynamic correction control effect, the control strategy of the projectile's correction mechanism is studied in this paper. A design method of trajectory correction control strategy based on particle swarm optimization-cuckoo search (PSO-CS) hybrid algorithm is proposed to obtain the optimal control parameters that can make the projectile flight stable and correct accurately. Firstly, the mathematical model of the air duct structure projectile is established. Secondly, the multiobjective optimization problem is analyzed. The projectile's correction control strategy optimization model is established by taking the start control time, the number of corrections, the correction working time, and the interval time as the control variables. The optimization model innovatively considers the influence of the correction action on the flight stability of the projectile and the influence of the start control time on the correction range. Finally, the PSO-CS hybrid algorithm is used to design the calculation method of the optimization model and solve the optimal correction working parameters. The simulation results indicate that the control strategy optimization model can be solved by the proposed calculation method. Moreover, optimal correction working parameters of the correction mechanism in the current state can be obtained. Compared with the results of using single PSO algorithm and CS algorithm, the correction scheme calculated by PSO-CS hybrid optimization algorithm is better. This correction control scheme can effectively reduce the impact point deviation and make the projectile flight stable. At the same time, the circular error probable (CEP) of the projectile after correction is reduced from 42.3 m to 4.6 m while the impact point dispersion is lowered. The research results show that the design method of correction control strategy proposed in this paper is effective for trajectory correction of the new air duct structure projectile.

1. Introduction

Modern warfare places increasing demands on the firing accuracy of weapons. In the process of firing and flying, conventional projectiles have low hitting accuracy due to the influence of various disturbances. The trajectory correction projectile is based on the conventional projectile with the addition of the correction mechanism. The correction mechanism can perform the corrective action based on the deviation between the projectile and the ideal trajectory in flight. Consequently, the projectile's aerodynamic force and moment are altered to achieve trajectory correction. The trajectory correction projectile can improve operational effectiveness and reduce collateral damage, meeting the requirements of a high cost-effectiveness ratio in modern warfare. Therefore, in recent years, trajectory correction technology has been one of the key research directions in intelligent ammunition.

The commonly used correction mechanisms for existing trajectory correction projectiles are umbrella resistance correction fuses, pulse detonation engines, and fixed canards. The umbrella resistance correction fuse can only achieve one-dimensional motion direction correction of the projectile. The pulse detonation engine and fixed canard correct the projectile in the two-dimensional motion direction. The pulse detonation engine is mainly used for mortars to

initiate the explosive device. However, the safety of the pulse detonation engine is poor. The correction technology of the fixed canard, such as the Precision Guidance Kit (PGK), is relatively difficult [1–4]. This method achieves trajectory correction by reducing the rotation speed of the rudder and controlling the canard roll angle. However, the aerodynamic control force and moment generated by the fixed canards at the front end of the projectile can change the flight attitude (angle-of-attack). This, in turn, can affect the flight stability of the projectile [5–7].

In aerodynamic control methods of the trajectory correction projectile, the ram air control method takes the oncoming high-speed airflow during the projectile flight as the correction power source. The airflow impulse is used to correct the flight direction of the projectile. Few types of research and applications can be found regarding the research of trajectory correction projectiles using this correction method. Public information shows that Chandgadkar et al. [8] applied the ram air control mechanism to a fin-stabilized penetrator projectile. The results indicate that this correction mechanism can provide sufficient control force and reduce the dispersion of a direct-fire projectile.

In reference [9], we proposed an innovative correction scheme based on [8] with the controllable air duct structure for spin-stabilized projectiles. The projectile structure of this scheme adds internal air ducts based on the original conventional spinning projectile. The oncoming airflow is introduced from the air inlet to the middle of the projectile, while the air exit ports are arranged near the mass center. As the projectile rotates, the oncoming airflow entering internal air ducts can be derived through multiple air outlets. The outlet direction of the airflow is controlled by controlling the working state of the internal air valve, i.e., the correction direction is controlled. Thus, a 2D trajectory correction of the projectile can be achieved [10]. This correction scheme is relatively simple and safe. In this paper, the control strategy of the correction control system for the new spin-stabilized projectile with air duct structure is designed based on [9]. Lastly, a specific optimization method for correcting control parameters is proposed.

The projectile correction control system's design is the key to achieving trajectory correction and flight stability. Burchett and Costello [11] investigated using a small number of short-duration lateral pulses acting as a control mechanism to reduce the impact point dispersion of a direct-fire rocket. A unique control law is investigated that combines model predictive control and linear projectile theory for lateral pulse jet control. Cao et al. [12] presented an optimization strategy of firing phase angle control for an impulsive correction projectile that can minimize the number of pulse jets required to correct the residual trajectory deviation. Based on the study of impulsive correction projectile, Gao et al. [13] proposed an optimal control strategy for the firing control of the impulse thruster. The strategy considers the difference of longitudinal and horizontal correction efficiency, firing delay, roll rate, and flight stability. Inspired by the above literature, we propose a design method of correction control strategy suitable for the correction mechanism of the new air duct structure projectile. The optimal correction scheme is calculated to realize projectile trajectory correction and stable flight.

In recent years, intelligent algorithms have been applied to research aircraft control systems. Burchett [14] used a genetic algorithm to optimize the design variables of the rocket pulse jet controller. Gui et al. [15] proposed a new parameter optimization design method using an improved particle swarm optimization algorithm to solve a class of reaction control system problems for maneuverable reentry vehicles. It can be seen that the intelligent algorithms show a good optimization calculation effect.

Particle swarm optimization (PSO) is a random optimization method based on swarm intelligence [16]. This type of optimization is characterized by the advantages such as simple principle, low number of parameters, and global optimization. It has been widely used in many different fields, such as optimizing model parameters [17], processing feature selection problems [18], and solving multimodal optimization problems [19]. The PSO algorithm shows good optimization ability while solving complex optimization problems.

Furthermore, the PSO has been widely used in the optimal design calculation of projectile correction control parameters. Yang et al. [20] proposed a new approach to the fuel-optimal impulsive control problem of the guided projectile using an improved PSO technique. The appropriate impulse time, impulse action angle, and working impulse number can be calculated to minimize the pulse energy consumption. Sun et al. and Yang et al. [21, 22] presented a new parametric optimization approach based on a modified PSO algorithm for the control system of an impulsive-correction projectile. By using this method, the optimal number of impulses and the impulse interval time can be obtained to minimize the trajectory deviation.

However, the conventional PSO algorithm can easily fall into the local optimum. Researchers have proposed several improvement methods to improve the performance of this algorithm [23, 24]. Cuckoo search (CS) is a mathematical optimization algorithm inspired by the nesting and parasitic reproduction behaviors of some cuckoo species and the Lévy flight behavior of some fruit flies and birds [25, 26]. It has been successfully applied to solve various optimization problems because of its few parameters and easy implementation [27, 28]. The CS algorithm uses Lévy flight to generate a new solution. The randomness of Lévy flight makes the search process spread throughout the whole search space, which makes the global search ability of the algorithm stronger. The CS algorithm, a relatively new metaheuristic search algorithm, has been extensively studied and discussed on the fusion and improvement with the PSO algorithm [29, 30].

At present, the PSO algorithm is mainly used to optimize the control strategy design of the existing trajectory correction projectile [20–22]. However, the fusion of the PSO and CS algorithms can make up for the shortcomings of their respective algorithms and improve the calculation accuracy. In this paper, we innovatively use the PSO-CS hybrid optimization algorithm to solve the optimization problem of the projectile correction control strategy and propose an optimization design method of the correction control parameters suitable for the air duct structure

projectile. Through simulation and comparison, it is shown that the correction scheme calculated by the PSO-CS algorithm is better than the single algorithm.

At the same time, it can be seen from the above literature that fewer design variables have to be considered in the optimal design of impulsive correction projectile control parameters. Due to the different correction principles, the existing control parameter optimization methods of impulsive correction projectile cannot be fully applied to the control parameter design of the new air duct structure projectile.

The correction force is affected by the oncoming airflow velocity and flight time during the correction of the spin-stabilized projectile with air duct structure. At the same time, parameters such as the start control time, number of corrections, correction working time, and interval time also directly affect the final trajectory correction effect. By controlling and optimizing the correction parameters [31, 32], the formed correction force can be mainly used to achieve projectile translation in a two-dimensional direction. Thus, a large overturn moment can be avoided while achieving the optimal correction effect. Consequently, the projectile still has good flight stability in the correction section.

The relationship between projectile flight aerodynamic parameters and correction working parameters was deduced in [9]. Under the condition of stable flight, the range of the correction action's working time and interval time was studied. However, the correction control parameters were not optimized. In this paper, we further study the correction control strategy applicable to the new air duct structure projectile based on [9] and the optimization design method of the control parameters.

The contributions of this paper are twofold.

(1) An optimization model of trajectory correction control strategy suitable for a new air duct structure projectile is proposed. The model considers the influence of the correction action on the flight stability of the projectile and the influence of the start control time on the correction range. The optimal correction working mode that minimizes the impact point deviation and the total number of corrections and optimizes the start control time can be obtained

(2) A model calculation method based on the PSO-CS hybrid algorithm is proposed to solve the optimization model of the control strategy and determine the optimal correction working parameters of the projectile correction mechanism

In this paper, the correction principle of the new air duct structure projectile is analyzed, and the mathematical model of the projectile is established. Then, the optimization model for the trajectory correction control strategy is established by taking the start control time, number of corrections, correction working time, and interval time as the correction control variables. Furthermore, the PSO-CS hybrid algorithm is used to design the calculation method of the optimization model and solve the optimal working parameters of the correction mechanism. Finally, the model is simulated and calculated by the PSO-CS hybrid algorithm. The validity of the proposed optimization design method of control strategy for trajectory correction of the projectile is verified by using the calculated optimal correction working parameters to simulate the trajectory impact point of the controlled projectile.

2. Air Duct Structure Projectile Mathematical Model

2.1. Correction Principle of the Projectile. The shape structure of a spin-stabilized trajectory correction projectile with the air duct structure in the uncorrected configuration is shown in Figure 1. The aerodynamic shape of the projectile is almost the same as the conventional projectile shape. The external shape and internal air duct structure of the projectile in the corrected configuration are shown in Figure 2. The air ducts are composed of a single inlet and three outlets evenly distributed along the circumference (air outlets I, II, and III are shown in Figure 2). When the air duct structure projectile enters the correction state, the false cap at the front end of the projectile is unlocked, and the air inlet is opened. The oncoming airflow is introduced from the air inlet to the air valve in the middle of the projectile. A corresponding airflow channel is present inside the air valve.

The projectile control system determines the correct direction according to the current position relative to the ideal trajectory and obtains the trajectory deviation value from the trajectory deviation solving system. Secondly, the control system generates the optimal control strategy according to the current flight state and guides the internal air valve correction mechanism to start the corrective action. By reasonably controlling the rotation speed of the air valve, the internal and external air ducts can flow air in the correction direction as the projectile rotates. Lastly, a two-dimensional impulse with a fixed direction is formed to provide the control force and the moment required for trajectory correction.

2.2. Mathematical Model of the Projectile. The lateral aerodynamic correction force F_p of the new air duct structure projectile is generated by the oncoming airflow, which is affected by the changes in the airflow rate. According to the momentum theorem, the air jet impulse I_p at the exit port can be expressed as follows:

$$I_p = F_p \cdot \Delta t = m_{\text{air}} \cdot v_{\text{air}}, \tag{1}$$

where m_{air} is the air mass flowing out of the exit port during the correction time Δt and v_{air} is the airflow rate at the exit port. The correction force F_p can be expressed as follows:

$$F_p = m_{\text{air}} \cdot \dot{v}_{\text{air}} = \int_0^{\Delta t} q_m dt \cdot \dot{v}_{\text{air}}, \tag{2}$$

$$q_m = \rho \cdot q_v = \rho \cdot v_{\text{air}} \cdot A = \rho \cdot v_{\text{air}} \cdot \frac{\pi}{4} d^2, \tag{3}$$

where ρ is the air density, q_m is the mass flow, q_v is the flow rate, A is the cross-sectional area of the duct, and d is the inlet diameter.

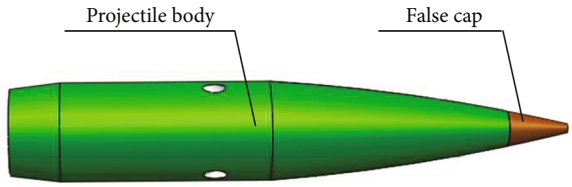

Figure 1: Projectile structure schematic for the uncorrected configuration.

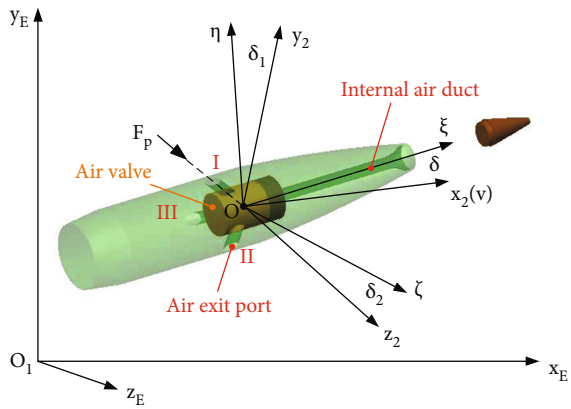

Figure 2: Projectile structure schematic for the corrected configuration and projectile's position definition.

2.2.1. Dynamic Equation of the Projectile. Relevant coordinate frames of the new air duct structure projectile are established [33–35]. The velocity coordinate frame is used as a reference to study the projectile mass center motion and calculate aerodynamics. The axis coordinate frame is used as a reference to study the projectile motion around the mass center and calculate the moment. The ground coordinate frame is used as a reference to describe the flight trajectory of the projectile. The velocity coordinate frame $Ox_2y_2z_2$, axis coordinate frame $O\xi\eta\zeta$, and ground coordinate frame O_1 $x_Ey_Ez_E$ are shown in Figure 2.

In the uncorrected configuration, the projectile in flight is affected by the gravity, drag, lift, Magnus force, damping moment, equatorial damping moment, pitching moment, Magnus moment, and gyroscopic moment. In the corrected configuration, the new air duct structure projectile is additionally affected by the lateral aerodynamic correction force F_p and the correction moment M_p based on the stable flight. The translational kinematic equation and dynamic rotational equation of the projectile in the corrected configuration are given by

$$\begin{cases} \dfrac{dv}{dt} = \dfrac{F_{x2} + F_{px2}}{m}, \\ \dfrac{d\theta_a}{dt} = \dfrac{F_{y2} + F_{py2}}{mv\cos\psi_2}, \\ \dfrac{d\psi_2}{dt} = \dfrac{F_{z2} + F_{pz2}}{mv}, \end{cases} \tag{4}$$

$$\begin{cases} \dfrac{d\omega_\xi}{dt} = \dfrac{M_\xi + M_{p\xi}}{J}, \\ \dfrac{d\omega_\eta}{dt} = \dfrac{M_\eta + M_{p\eta}}{I} - \dfrac{J\omega_\xi\omega_\zeta}{I} + \omega_\zeta^2 \tan\varphi_2, \\ \dfrac{d\omega_\zeta}{dt} = \dfrac{M_\zeta + M_{p\zeta}}{I} + \dfrac{J\omega_\xi\omega_\eta}{I} - \omega_\eta\omega_\zeta \tan\varphi_2, \end{cases} \tag{5}$$

where m is the projectile quality; v is the flight velocity; F_{x2}, F_{y2}, and F_{z2} are components of the aerodynamic force of the projectile on each axis in the velocity coordinate before the correction; and F_{px2}, F_{py2}, and F_{pz2} represent correction force components in the velocity coordinate. Parameters θ_a and ψ_2 represent elevation angle and velocity azimuth angle, respectively; M_ξ, M_η, and M_ζ are the moment components on each axis within the axis coordinate before the correction; and $M_{p\xi}$, $M_{p\eta}$, and $M_{p\zeta}$ represent correction moment components in the axis coordinate. Parameters ω_ξ, ω_η, and ω_ζ are the rotational angular velocities of the projectile on each axis, J and I represent the axial and equatorial moments of inertia, respectively, and φ_2 is the axis azimuth angle.

2.2.2. Angle-of-Attack Equation of the Projectile. According to Equations (4) and (5), the corresponding force and moment expressions [9] are substituted, and the variation equation of the complex angle-of-attack of the projectile with arc length in the corrected configuration can be obtained as follows:

$$\begin{aligned} &\Delta'' + (H - iP)\Delta' - (M + iPT)\Delta \\ &\quad = -\frac{\ddot{\theta}}{v^2} - (k_{zz} - iP)\frac{\dot{\theta}}{v} - i\cdot\frac{M_{p\eta} + iM_{p\zeta}}{Iv^2} + \frac{F_{py_2} + \mathrm{i}F_{pz_2}}{mv^2} \\ &\qquad \cdot\left(iP - k_{zz} - b_x - \frac{g\sin\theta}{v^2}\right). \end{aligned} \tag{6}$$

The related parameters are shown in

$$\begin{cases} H = k_{zz} + b_y - b_x - \dfrac{g\sin\theta}{v^2}, \\ P = \dfrac{J\dot{\gamma}}{Iv}, \\ M = k_z, \\ T = b_y - \left(\dfrac{I}{J}\right)k_y, \end{cases} \tag{7}$$

where θ is the trajectory inclination angle, $\dot{\gamma}$ is the angular velocity, b_x and b_y are the relevant parameters of the drag coefficient and lift coefficient, respectively, and k_y, k_z, and k_{zz} are the relevant parameters of the Magnus moment coefficient, pitching moment coefficient, and equatorial damping moment coefficient, respectively.

The homogeneous solution of the angle-of-attack equation represents angular motion under the initial condition. The instantaneous state after correction is taken as the initial

condition. The homogeneous solution is obtained as follows:

$$\Delta = C_1 e^{(\lambda_1 + i\omega_1)s} + C_2 e^{(\lambda_2 + i\omega_2)s}. \quad (8)$$

According to the homogeneous solution of the angle-of-attack equation, the projectile's motion is represented by a complex motion of two vectors. Here, C_1 and C_2 are complex undetermined constants determined by initial conditions, λ_1 and λ_2 are the damping indexes, and ω_1 and ω_2 are modal frequencies.

2.2.3. Flight Motion Equation of the Projectile. When the control system performs trajectory simulation and predicts the impact point position, the 4-DOF model of the air duct structure projectile is used for calculation. The changes in displacement, velocity, and angular velocity of the projectile are studied within the ground coordinate frame $O_1 x_E y_E z_E$. The 4-DOF equation is shown in

$$\begin{cases} \dfrac{dv_x}{dt} = \dfrac{R_{x_{vx}} + R_{y_{vx}} + R_{z_{vx}} + F_{p_{vx}}}{m} + g_x, \\ \dfrac{dv_y}{dt} = \dfrac{R_{x_{vy}} + R_{y_{vy}} + R_{z_{vy}} + F_{p_{vy}}}{m} + g_y, \\ \dfrac{dv_z}{dt} = \dfrac{R_{x_{vz}} + R_{y_{vz}} + R_{z_{vz}} + F_{p_{vz}}}{m} + g_z, \\ \dfrac{dx}{dt} = v_x, \\ \dfrac{dy}{dt} = v_y, \\ \dfrac{dz}{dt} = v_z, \\ \dfrac{d\dot{\gamma}}{dt} = -k_{xz} \cdot v_r \cdot \dot{\gamma}, \end{cases} \quad (9)$$

where x, y, and z represent the projectile's position in the ground coordinate frame; R_x, R_y, R_z, and g represent the drag, lift, Magnus force, and gravitational acceleration; and k_{xz} is the relevant parameter of the damping moment coefficient.

If the effect of wind disturbance is accounted for, the absolute velocity v of the projectile can be regarded as the vector sum of the velocity v_r relative to the air stream and the wind velocity W, i.e., $v = v_r + W$.

$$v_r = \sqrt{(v_x - W_x)^2 + v_y^2 + (v_z - W_z)^2}. \quad (10)$$

3. Optimization Model Design of the Correction Control Strategy

3.1. The Process of Trajectory Correction Control. During the flight of the air duct structure projectile, the controller detects the projectile's real-time position and attitude information through GPS and geomagnetic sensors. The received data is processed by the DSP. Then, the trajectory model is used to calculate and simulate the actual flight trajectory of the projectile and the impact point position in the uncontrolled state. The trajectory deviation value E can be calculated by the comparison with the preset standard trajectory and target position, as shown in Figure 3. Here, R_T is the target vector, and R_C is the predicted impact point position vector, $E = R_C - R_T$.

It is assumed that parameter ΔE_{a0} represents the projectile's allowable impact point deviation value. Then, a circle is drawn with the target position as the center and the radius $\Delta E_{a0} = \varepsilon_0$. When the impact point deviation value is higher than the allowable value ε_0 set by the system, the impact point of the projectile in the uncontrolled state is outside the circle. Then, the deviation signal is converted into a design start signal for the trajectory correction control strategy. This moment is set to t_{a0}. The projectile is not corrected if the impact point deviation value is within the threshold range. The control system performs calculations according to the optimization model of the correction strategy, forms an optimal control scheme, determines the corrected working parameters of the air valve, and obtains the control command.

When the calculated optimal start control time t_a is reached, the false cap at the front end of the projectile is unlocked, and the projectile starts to enter the corrected working state. If the flight does not reach the start control time t_a, the flight motion equation is updated, and the control scheme is recalculated. The optimal correction control strategy calculated by the algorithm is used to guide the work of the air valve and control the projectile to fly to the target and achieve trajectory correction. The control system working process of the air duct structure projectile is shown in Figure 4.

3.2. Optimization Model of the Correction Control Strategy. The air duct structure projectile can be corrected several times through the air valve work in the corrected state. In this paper, an optimization model of trajectory correction control strategy is established by analyzing the multiobjective optimization problem. According to the flight motion equation of the projectile, the combination of correction parameters that minimize the objective function is calculated to form the optimal correction control strategy. Thus, the projectile can be guided to gradually fly to the target through multiple corrections and achieve the optimal control effect.

3.2.1. Objective Function and Design Variables. The main control goal is to reduce the deviation between the impact point position of the projectile and the target through multiple corrections. However, according to Equation (6), the lateral jet's correction action changes the projectile's flight angle-of-attack. In other words, each correction may affect the flight stability of the projectile. Hence, the number of corrections should not be excessive. At the same time, considering the influence of algorithm calculation time on the real-time performance of the correction, the correction strategy adopts a one-time decision. The correction feedback is not done in real time after the starting control. However, wind disturbance and other factors may cause new trajectory deviation. The interval between the start control time and

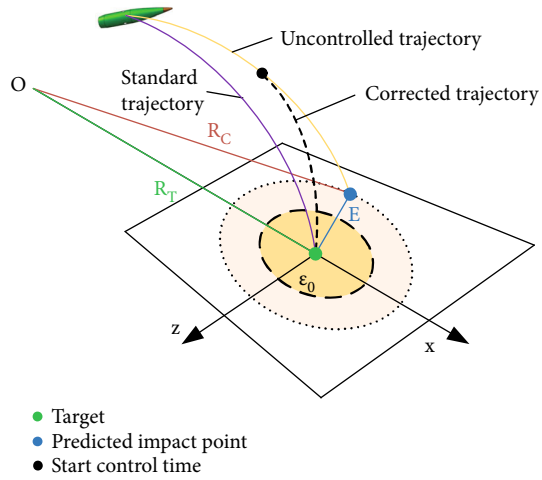

Figure 3: Schematic of the projectile correction process.

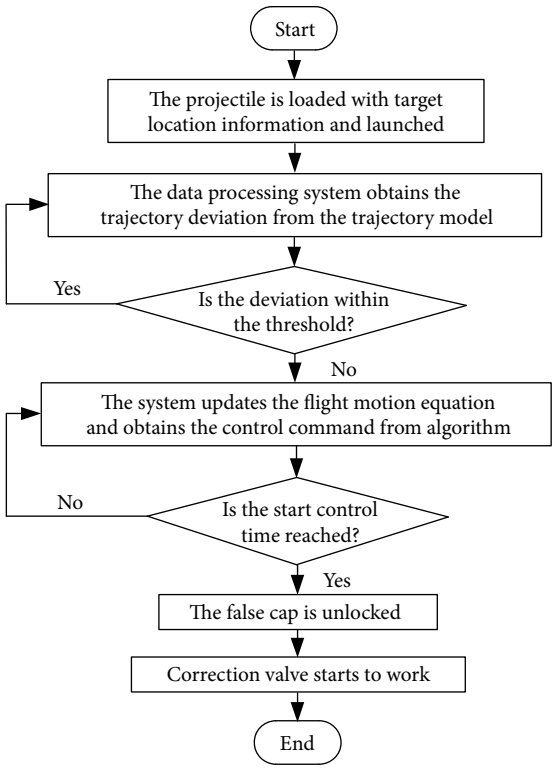

Figure 4: The working process of the projectile's control system.

the design start moment of the correction strategy is conducive to the accumulation of various system errors. Therefore, it is necessary to consider the setting of the start control time t_a to make the correction range as large as possible. Thus, the correction ability of the projectile can be fully used.

In this paper, the multiobjective optimization method is used to design the trajectory correction control strategy of the air duct structure projectile. The strategy designed by this method ensures that the impact point deviation of the projectile is as small as possible, the number of corrections is least, and the start control time is the latest, i.e., the cumulative trajectory deviation corresponding to the start control time is the largest. This forms a multiobjective optimization problem with the impact point deviation ΔE, the number of corrections n, and the trajectory deviation ΔP corresponding to the t_a time as the optimization target.

However, increasing the number of corrections can improve the correction accuracy of the projectile, but it also increases the adverse effect on flight stability. The later the start control time is, the greater the cumulative trajectory deviation. To a certain extent, this increases the number of corrections and the impact point deviation. The weighted sum of each objective is performed and transformed into a function f to coordinate the contradictions of the three optimization objectives.

The objective function f can be written as

$$\min f = k_1 \cdot \frac{n}{n_{\max}} + k_2 \cdot \frac{\Delta E}{\Delta E_{a0}} + k_3 \cdot \frac{\Delta E_{a0}}{\Delta P}, \tag{11}$$

where $n_{\max}$ is the maximum number of corrections that the projectile can make, ΔE is the deviation between the impact point of the projectile and the target after correction, ΔP indicates the magnitude of the trajectory deviation corresponding to the start control time, and k represents the proportional factor of different objectives in the optimization algorithm (k is a positive value). min f is the minimum value that solves for the linear combination of the three optimization objectives.

It is assumed that the position coordinate of the target is $(x_{\text{target}}, z_{\text{target}})$. At the moment t_a, the position coordinate of the projectile in the standard trajectory is (x_{ta}, z_{ta}), and the position coordinate after disturbance is (x'_{ta}, z'_{ta}). The impact point coordinate of the corrected projectile is (x_c, z_c). Then, the impact point deviation ΔE of the corrected projectile and the trajectory deviation ΔP at moment t_a can be expressed as follows:

$$\Delta E = \sqrt{\left(x_c - x_{\text{target}}\right)^2 + \left(z_c - z_{\text{target}}\right)^2}, \tag{12}$$

$$\Delta P = \sqrt{\left(x'_{ta} - x_{ta}\right)^2 + \left(z'_{ta} - z_{ta}\right)^2}. \tag{13}$$

The trajectory correction effect of air duct structure projectile is affected by many factors. Under the corrected configuration, the correction impulse is generated by the oncoming airflow. According to Equations (1)–(3), the impulse magnitude is determined by the jet velocity at the exit port and the correction working time. However, the lateral jet velocity is related to the start control time. Affected by flight drag, the earlier the start control time, the faster the projectile flies, the greater the lateral correction force formed, and the stronger the correction ability. At the same time, the trajectory correction effect needs to consider the flight stability of the projectile. The number of corrections, correction working time, and interval time between multiple corrections affects the flight angle-of-attack of the projectile.

In this paper, the main correction parameters that affect the trajectory correction effect in the design of the correction control strategy are optimized. The start control time t_a,

number of corrections n, single correction working time Δt, and interval time ΔT between two adjacent correction actions are selected as design variables. The objective function f is solved by substituting design variables into the flight motion equation of the projectile. Calculating the set of correction parameter combinations (t_a, Δt_1, ΔT_1, …, ΔT_{n-1}, Δt_n) that minimizes the objective function value is the optimal trajectory correction strategy for the projectile.

3.2.2. Flight Constraints. The correction parameters must be limited during the correction process of the air duct structure projectile to maintain a stable flight, control the correction accuracy, and improve the correction range. The specific analysis is as follows.

(1) Amplitude of Angle-of-Attack Increment. If the angle-of-attack caused by the correction action is too large during the projectile correction, the projectile may become unstable. Flight stability of the projectile during correction can be ensured if the amplitude of the angle-of-attack increment $\Delta\delta$ caused by each correction action does not exceed the limited allowable value $\Delta\delta_{\max}$:

$$\Delta\delta \le \Delta\delta_{\max}. \tag{14}$$

(2) Correction Working Time and Interval Time. The appropriate range of the correction working time Δt can be calculated by limiting the change in the angle-of-attack caused by each correction to a certain range. According to Equations (4) and (5), the motion state of the projectile changes suddenly after the lateral correction action. The projectile angle-of-attack increment $\Delta\delta$ produced by the correction action can be calculated as follows:

$$\Delta\delta = \left|\frac{F_p \cdot \Delta t}{mv\sqrt{\sigma}}\right| + \left|\frac{F_p \cdot \Delta t \cdot L_p}{I\alpha v\sqrt{\sigma}}\right|, \tag{15}$$

where L_p is the axial distance between the center of the air jet at the exit port and the mass center of the projectile, $\sigma = 1 - k_z/\alpha^2$, and $\alpha = J\dot{\gamma}/(2Iv)$. The projectile angle-of-attack increment $\Delta\delta$ must be lower than the limited allowable value $\Delta\delta_{\max}$ to maintain stable flight. The constraint can be obtained by substituting Equations (1)–(3) and simplified as follows:

$$\Delta t < \frac{\Delta\delta_{\max}}{\left|F_p/mv\sqrt{\sigma}\right| + \left|\left(F_p \cdot L_p\right)/I\alpha v\sqrt{\sigma}\right|} \approx \frac{\Delta\delta_{\max}}{\left|\left(\rho \cdot v_{\text{air}} \cdot L_p\right)/I\alpha\sqrt{\sigma} \cdot (\pi/4)d^2\right|}. \tag{16}$$

In this paper, the velocity loss of the airflow through the interior of the projectile is not considered, i.e., $v_{\text{air}} \approx v$. When the allowable value $\Delta\delta_{\max}$ is fixed, the velocity of the lateral jet is inversely proportional to the correction working time. In other words, the greater the air jet velocity, the less time it takes for the correction action to form the same angle-of-attack. When the projectile is in the design stage of the correction strategy, the maximum flight velocity is at the moment t_{a0}. If the correction is performed at this moment, the corresponding correction working time is minimal and set to $\Delta t_{\min}$.

When the single correction working time Δt is determined, the disturbance value $\Delta\delta$ caused by the correction action on the projectile's angle-of-attack can be calculated via Equation (15). When the correction is paused, the angle-of-attack increment tends to stabilize under the action of the gyroscopic moment and equatorial damping moment. The damping index λ is used for calculation. Assuming that the first correction action is completed at time t_1, the angle-of-attack increment is continuously reduced due to damping. In the period ΔT between two adjacent correction actions, the attenuation of the attack angle can be represented as follows:

$$b = \Delta\delta e^{\lambda s(t_1)} - \Delta\delta e^{\lambda s(t_1+\Delta T)}. \tag{17}$$

The interval between two adjacent correction actions should ensure that the angle-of-attack increment has enough attenuation time to maintain flight stability. When the angle-of-attack increment decreases to less than $1/a$ of the original increment, i.e., $b > (a-1)\,\Delta\delta/a$, the angle-of-attack is stabilized. Then, subsequent corrections can be carried out. Therefore, the interval time between two correction actions is provided as follows:

$$\Delta T > \frac{1}{\lambda} \ln\left(e^{\lambda s(t_1)} - \frac{a-1}{a}\right) - t_1 = \Delta T_{\min}. \tag{18}$$

(3) The Number of Corrections. Since the correction action impacts the flight stability of the projectile, it is necessary to limit the number of corrections n, which cannot be higher than the maximum number of corrections. The number of corrections n should satisfy the following inequality:

$$n < n_{\max} = \frac{t_{\text{total}} - t_{a0}}{\Delta t_{\min} + \Delta T_{\min}}, \tag{19}$$

where t_{total} is the total flight time of the projectile.

(4) The Start Control Time. The earlier the correction start control time, the higher the flight velocity and the greater the correction force formed. The late start control time is conducive to accumulating various errors in the system. However, the correction ability of the projectile will be reduced. At the same time, the angular velocity $\dot{\gamma}$ of the projectile decreases with an increase in the flight time, which directly affects the gyro stability of the spinning projectile. Therefore, the start control time cannot be too late considering the correction ability and flight stability when the air duct structure projectile is in the corrected state. By limiting the minimum value of $\dot{\gamma}$, the projectile is required to correct before the angular velocity decreases to $\dot{\gamma}_{\min}$. Then, the constraint on the start control time t_a can be written as

$$t_{a0} \le t_a \le t_{a\,\max}, \tag{20}$$

where t_{amax} is the corresponding time when the angular velocity of the projectile changes to $\dot{\gamma}_{\min}$.

(5) The Correction Accuracy. The correction action requires the projectile to achieve a certain correction accuracy. In other words, the impact point deviation ΔE of the projectile cannot be too large. The inequality constraint is as follows:

$$\Delta E \le \Delta E_{a0}. \tag{21}$$

3.2.3. Control Strategy Optimization Model. To sum up, the optimization model of the trajectory correction control strategy of a new air duct structure projectile can be expressed as follows:

$$\begin{cases} \min f(t_a, n, \Delta t, \Delta T) = k_1 \cdot \dfrac{n}{n_{\max}} + k_2 \cdot \dfrac{\Delta E}{\Delta E_{a0}} + k_3 \cdot \dfrac{\Delta E_{a0}}{\Delta P} \\ \text{s.t.} g_i(x) \le 0, \end{cases} \tag{22}$$

where x is the decision vector and $g_i(x)$ represents the inequality constraints in the optimization model. The design variables in the optimization model represented by Equation (22) include both continuous and discrete integer variables. In Chapter 4, we use the PSO-CS hybrid algorithm to optimize the model and use the step-by-step optimization method to design a specific calculation method.

4. Calculation Method of Correction Control Strategy Model

4.1. PSO-CS Hybrid Algorithm

4.1.1. PSO Algorithm. PSO algorithm is a random intelligent optimization algorithm proposed by Eberhart and Kennedy. In this algorithm, each particle represents a single optimization problem solution. Each particle is assumed to have two characteristics: position and velocity; all particles form a swarm. The particles comprehensively adjust their flight velocities according to their experience and group knowledge. Thus, they gradually approach the position of the optimal swarm solution.

The PSO algorithm first randomly initializes the position and velocity of particles in the solution space, calculates the fitness values of the particles, and enters the iterative update of the algorithm. Assume that the problem is solved in a D-dimensional search space. The swarm consists of N particles, expressed as Swarm $= \{x_1^{(u)}, x_2^{(u)}, \cdots, x_N^{(u)}\}$. Parameter u represents the iteration counter. The position of the i-th particle is denoted as $X_i = (x_{i1}, x_{i2}, \cdots, x_{id}, \cdots, x_{iD})$, and the corresponding velocity is denoted as $V_i = (v_{i1}, v_{i2}, \cdots, v_{id}, \cdots, v_{iD})$, $i = 1, 2, \cdots, N$. The individual optimal position of the i-th particle is expressed as $p_i = (p_{i1}, p_{i2}, \cdots, p_{id}, \cdots, p_{iD})$. The optimal swarm position is expressed as $p_g = (p_{g1}, p_{g2}, \cdots, p_{gd}, \cdots, p_{gD})$. During the iteration, particle i updates its position and velocity according to the following equation:

$$\begin{cases} v_{id}^{(u+1)} = \omega \cdot v_{id}^{(u)} + c_1 r_1 \left(p_{id}^{(u)} - x_{id}^{(u)}\right) + c_2 r_2 \left(p_{gd}^{(u)} - x_{id}^{(u)}\right), \\ x_{id}^{(u+1)} = x_{id}^{(u)} + v_{id}^{(u+1)}, \end{cases} \tag{23}$$

where ω is the inertia weight, c_1 and c_2 are the acceleration factors, and r_1 and r_2 are random numbers between [0, 1]. The search velocity range of each particle is $[v_{\min}, v_{\max}]$, and the position range is $[x_{\min}, x_{\max}]$. The algorithm updates the particles through Equation (23) to complete the optimization calculation.

4.1.2. CS Algorithm. The CS is a new intelligent optimization algorithm proposed by Yang and Deb [36, 37] and based on the cuckoo randomly searching for the nest to lay eggs and Lévy flights. It is based on three idealized rules:

(1) Each cuckoo lays one egg at a time and dumps its egg in a randomly chosen nest

(2) The best nests with high-quality eggs (solutions) will carry over to the next generations

(3) The number of available host's nests is fixed, and the egg laid by a cuckoo is discovered by the host bird with a probability P_a ($P_a \in [0, 1]$). The worst nests are discovered and discarded from further calculations

In the CS algorithm, N host nests are first randomly initialized in the solution space. It is assumed that the location of the i-th nest in the D-dimensional search space is $e_i^{(u)}$. The best solutions are retained by evaluating the fitness of each nest. Then, the iterative process is started in a new nest location.

The CS is based on the three rules mentioned above and uses the following two methods to generate new solutions:

(1) The nest location is updated based on Lévy flights

$$e_i^{(u+1)} = e_i^{(u)} + \tau \oplus \text{Levy}(\lambda), \quad i = 1, 2, \cdots, N, \tag{24}$$

where $\tau > 0$ is the step size and the product $\oplus$ represents entry-wise multiplications. The Lévy flights Levy (λ) essentially provide a random walk

(2) The random number P is compared with the probability P_a. If $P > P_a$, the egg laid by a cuckoo is discovered. Then, the updated formula of the new nest location can be expressed as

$$e_i^{(u+1)} = e_i^{(u)} + r\left(e_j^{(u)} - e_i^{(u)}\right), \tag{25}$$

where r is a random number uniformly distributed in [0, 1]

and $e_j^{(u)}$ is a nest near $e_i^{(u)}$. Conversely, if the egg laid by a cuckoo is not found, the nest location is not updated.

4.1.3. PSO-CS Hybrid Algorithm Calculation Process. The PSO algorithm has a strong local search ability but is easily affected by the value of the inertia weight ω. It can be seen from Equation (23) that ω determines the change amplitude of the current particle velocity. The larger ω, the larger the search range of the solution. It can improve the global search ability of the algorithm. The smaller ω, the smaller the search range of the solution. It is easy to fall into local optimum, which makes the swarm lose the ability to explore. However, the CS algorithm uses Lévy flight. The randomness of Lévy flight makes the algorithm's local search ability poor. The CS algorithm focuses more on global exploration and has a strong ability to jump out of local search [38]. Therefore, combining the two algorithms can compensate for the shortcomings of their respective algorithms.

The entire calculation process of the PSO-CS hybrid algorithm is depicted in Figure 5. The specific steps are as follows:

(1) PSO initialization includes setting swarm size, iteration times, and inertia weight. The position and velocity of each particle are initialized

(2) The initial particle position is taken as the individual optimal position p_i of a particle. The fitness value of each particle is calculated from the fitness function f, and it is taken as the individual optimal fitness $f_{i\text{best}}$ of the particle. The position corresponding to the swarm optimal fitness $f_{g\text{best}}$ is the global optimal position p_g

(3) The position and velocity of each particle are updated according to Equation (23), and the fitness of each particle is calculated

(4) The individual optimal position p_i and the optimal global position p_g are updated for the current N particles. The current fitness of a particle is compared to the previous optimal fitness. If the current fitness is better, it is taken as the optimal fitness $f_{i\text{best}}$ of the particle, and the individual optimal position is updated. At the same time, the optimal fitness $f_{g\text{best}}$ and optimal global position of the entire population are updated by comparison

(5) The current global optimal position p_g is reserved, and the CS algorithm parameters are initialized. The individual optimal position combination $P_u = (p_1, p_2, \cdots, p_i, \cdots, p_N)^T$ of N particles is taken as the initial position of the CS. Then, the search enters the algorithm to continue iterative updates

(6) The location of the best nest of the previous generation is preserved. For other nests, Equation (24) is employed to update the location and calculate the fitness of each nest

(7) The operation that the host bird finds egg laid by a cuckoo is performed. If the random number P is greater than the probability P_a of being found by the host bird, the nest location is updated via Equation (25). Compared with the location before the update, the nest location $p_{i\text{new}}$ is replaced and retained with better fitness. At the same time, the global optimal location $p_{g\text{new}}$ is updated

(8) Evaluate whether the iteration termination conditions are met. If so, the global optimal position $p_{g\text{new}}$ is output, and the algorithm ends. Otherwise, return to step (3) and replace p_i and p_g with new individual optimal position $p_{i\text{new}}$ and global optimal position $p_{g\text{new}}$. Then, bring them into the iteration for calculation. In other words, the CS algorithm is used to improve individual and global optimal positions, as well as to guide the PSO algorithm iteration to quickly find the optimal solution

4.2. Calculation Method of Control Strategy Model Based on Optimization Algorithm. In this paper, the PSO-CS hybrid algorithm is used to calculate the correction control strategy model of the air duct structure projectile and obtain optimal correction working parameters. The specific calculation method is designed as follows:

(1) The position vector of a particle is composed of the start control time t_a, number of corrections n_i, single correction working time Δt_{ni}, and interval time ΔT_{ni}. The particle vector X can be written as

$$X = \begin{bmatrix} t_a \\ \Delta t_{n1} \\ \Delta T_{n2} \\ \vdots \\ \Delta T_{ni-1} \\ \Delta t_{ni} \end{bmatrix}_{2n_i \times 1} \tag{26}$$

(2) Before calculation, design variables are limited according to constraints

According to the analysis of flight constraints in Section 3.2.2, first, the limited allowable value $\Delta\delta_{\max}$ of the angle-of-attack increment caused by each correction action is set. The upper limit $\Delta t_{ni\,\max}$ of the single correction working time and the lower limit $\Delta T_{ni\,\min}$ of the correction interval time can be calculated by (16) and (18). Secondly, the allowable impact point deviation ΔE_{a0} of the projectile is set to determine the design start moment t_{a0} for the correction control strategy. Then, the upper limit $n_{\max}$ of the number of corrections can be calculated by

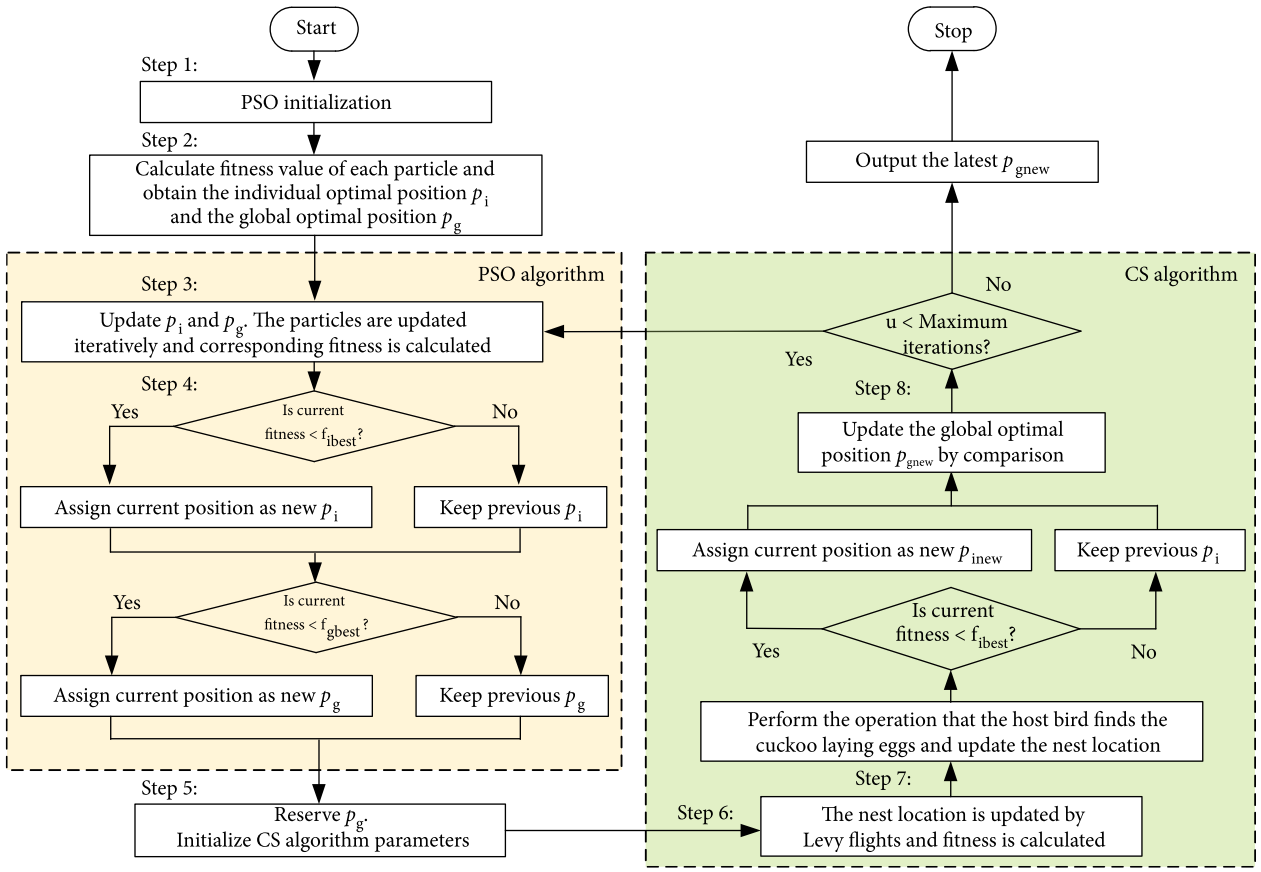

Figure 5: The calculation process of the PSO-CS hybrid algorithm.

(19). Finally, the angular velocity parameter $\dot{\gamma}_{\min}$ of the projectile is set, and the upper and lower limits of the start control time can be determined by (20).

(3) In the correction control strategy model of the projectile, the optimization objective function is a linear combination of the number of projectile corrections, the amount of impact point deviation, and the cumulative trajectory deviation corresponding to the start control time. In this paper, we design the calculation method of this objective function by using the step-by-step optimization method. The specific steps are as follows:

(a) The initial start control time t_0 is used for calculation. The PSO algorithm is used to determine the optimal number of corrections n_k

First, the initial start control time is set to t_0. The setting value of t_0 can be determined by multiple simulation experiments and satisfies the inequality constraint (20). The range of the projectile, the allowable impact point deviation, and the interference intensity are different, the corresponding initial start control time is different.

In order to improve the calculation efficiency and reduce the amount of calculation, the same interval time is set for multiple corrections, which is the minimum interval time $\Delta T_{n1\min}$ required after the first correction action. Affected by flight drag, the oncoming airflow velocity decreases with the increase of flight time, and the minimum interval time required for subsequent correction is less than $\Delta T_{n1\min}$. The projectile can fly stably under this setting conditions.

On this basis, the PSO algorithm is used for calculation. Because various particle dimensions are generated by the different number of corrections, $n_{\max} - 1$ swarms can be formed. Moreover, since different swarms use the same initial start control time in calculation, the corresponding trajectory deviation ΔP at moment t_0 is the same. Therefore, for setting the three proportional factors k of the objective function, set $k_3 = 0$. In this case, the objective function of the optimization calculation is

$$\min f_1 = k_1 \cdot \frac{n}{n_{\max}} + k_2 \cdot \frac{\Delta E}{\Delta E_{a0}}. \tag{27}$$

In the calculation process, when the impact point deviations of the projectile in different swarms are all within the range of ΔE_{a0}, in order to obtain the swarm of the particle with the minimum number of corrections and the minimum fitness of the objective function, k_1 and k_2 need to meet the following formula:

$$k_1 \cdot \frac{n_i - n_{i-1}}{n_{\max}} > k_2 \cdot \frac{\Delta E_{n_i} - \Delta E_{n_{i-1}}}{\Delta E_{a0}}. \tag{28}$$

For each swarm, randomly generate the N particles, and set the same iteration times. Update the position and velocity of each particle in the population according to Equation (23). The corresponding design variables are substituted into the projectile's flight motion equation, and each particle's fitness is calculated by Equation (27).

The $n_{\max} - 1$ swarms use the PSO algorithm and parallel computing method under the same conditions to search for the optimal particle in their respective swarms. By comparing and selecting the swarm n_k that contains the particle with the least fitness, then the optimal number of corrections is determined.

(b) The optimal number of corrections n_k is used for calculation. The PSO-CS algorithm is used to determine the optimal start control time t_a

After determining the optimal number of corrections, the PSO-CS algorithm is used to continue searching for the optimal particle of the swarm n_k. At this time, the start control time is not set, and the optimal particle is searched in the full range. In the proportional factor setting of the objective function, set $k_1 = 0$. Then, the objective function of the optimization calculation is

$$\min f_2 = k_2 \cdot \frac{\Delta E}{\Delta E_{a0}} + k_3 \cdot \frac{\Delta E_{a0}}{\Delta P}. \tag{29}$$

Unlike the previous step, which selects an optimal position among multiple populations, this step is calculated to select the optimal position in the same population. When the impact point deviation of the projectile is controlled within the range of ΔE_{a0}, in order to obtain the correction scheme with the optimal start control time, k_1 and k_2 need to meet the following formula:

$$k_2 \cdot \frac{\Delta E}{\Delta E_{a0}} < k_3 \cdot \frac{\Delta E_{a0}}{\Delta P}. \tag{30}$$

The particle with the least fitness can be calculated by the algorithm. Then, the correction scheme with the optimal start control time can be determined. The optimization process is shown in Figure 6.

(4) According to the algorithm calculation steps in Section 4.1.3, the global optimal position $p_{g\text{knew}}$ in the swarm n_k is finally output through iterative calculation, which can determine the optimal correction scheme with small impact point deviation, the least number of corrections, and the latest start control time. In other words, the optimal start control time, the number of corrections, the single correction working time, and the interval time of the corrected projectile in the current flight state are determined. Then, the calculation ends

In this section, we design an optimal scheme calculation method suitable for the trajectory correction control strategy

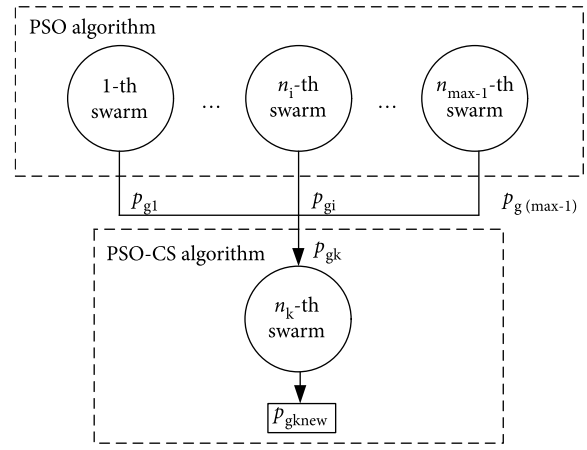

Figure 6: Schematic of an optimization process.

optimization model of the new air duct structure projectile by using the PSO-CS hybrid algorithm.

The step-by-step optimization method is adopted. Firstly, the PSO algorithm is used to determine the optimal number of corrections. The entire population is divided into several swarms according to the different number of corrections within the model. Through the parallel calculation of multiple swarms, the same initial start control time and correction interval time are set, and the optimal particle in multiple swarms is quickly found by using strong constraints. The swarm containing the optimal particle with the least fitness is selected among several swarms, and the optimal number of corrections is determined.

Secondly, the PSO-CS algorithm is used to determine the optimal start control time. The selected swarm continues to be calculated by using PSO-CS algorithm, and the correction scheme with the optimal start control time is determined. This method can greatly reduce the amount of calculation and improve the calculation efficiency. The CS algorithm is introduced into the PSO algorithm, which balances local and global search capabilities by using their respective advantages. At the same time, the hybrid algorithm can speed up convergence and improve algorithm accuracy.

5. Results and Discussion

In this paper, the 155 mm spin-stabilized trajectory correction projectile with air duct structure is selected as the research object. The flight trajectory model is simulated to verify the validity of the control strategy optimization design method for the projectile trajectory correction. The design variables are introduced into the flight motion equation of the projectile, and the calculation method of control strategy model based on optimization algorithm in Section 4.2 is used for calculation.

During calculation, the structural parameters of the air duct structure projectile are set as follows: $m = 45$ kg and $L_p = 0.015$ m. The initial motion parameters of the projectile are as follows: $v_{x0} = 295$ m/s, $v_{y0} = 295$ m/s, $v_{z0} = 10$ m/s, $x_0 = 0$ m, $y_0 = 0$ m, $z_0 = 0$ m, $\theta_0 = 45\circ$, and $\dot{\gamma} = 200$ r/s. The wind velocity is $W_x = -5$ m/s and $W_z = 5$ m/s.

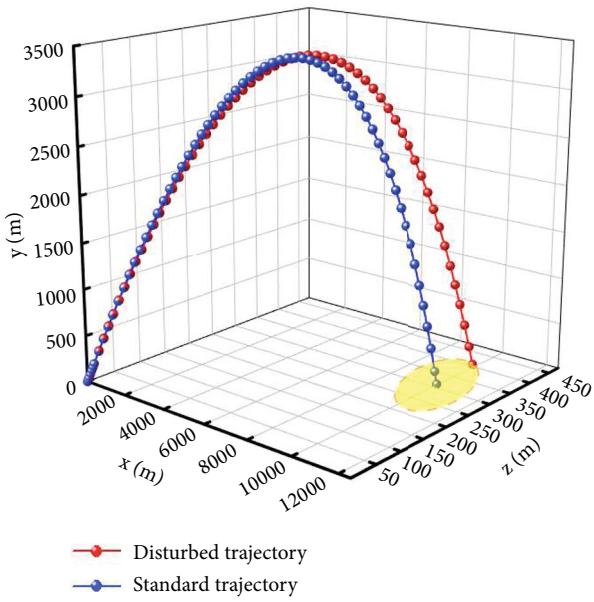

Figure 7: Trajectory comparison of the projectile with or without disturbance.

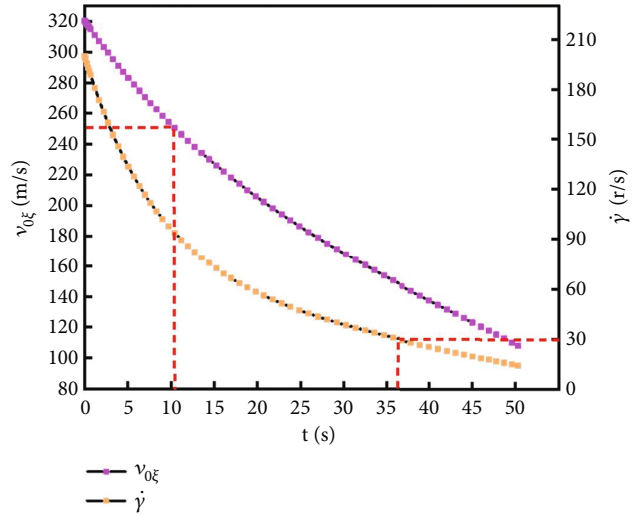

Figure 8: The change curves of the angular velocity and the flight velocity in the direction of the projectile's axis.

In the constraints of this optimization model, it is first necessary to set the limited allowable value $\Delta\delta_{\max}$ of the amplitude of the angle-of-attack increment. The size of this value can be adjusted according to the flight state of the projectile before the correction. Considering that manufacturing errors or other factors may lead to a large angle-of-attack caused by correction action, $\Delta\delta_{\max}$ is set to 8° [15, 21]. At the same time, the allowable impact point deviation ΔE_{a0} of the projectile is set to 10 m.

The flight trajectory of the projectile under different conditions can be obtained through simulation, as shown in Figure 7. Among them, the projectile's trajectory in the uncontrolled state and without wind disturbance represents the standard flight trajectory, as shown by the blue curve in the figure. Set the impact point position of this trajectory as the target position, $(x_{\text{target}}, z_{\text{target}}) = (9945.40, 312.14)$. The flight-disturbed trajectory of the projectile can be simulated according to the current disturbance conditions, as shown by the red curve in the figure.

Figure 8 simulates the change curve of the projectile angular velocity $\dot{\gamma}$ and flight velocity $v_{O\xi}$ of the projectile axis direction under the disturbance condition. The calculated total flight time is 50.30 s. When the trajectory deviation $\Delta E_{a0} = 10$ m corresponds to the moment $t_{a0} = 10.25$ s, the flight velocity of the projectile is $v_{O\xi a0} = 251.56$ m/s. It is assumed that the projectile must be corrected when the angular velocity is reduced to 30 r/s. It can be calculated that the constraint of the start control time t_a is $10.25\,\text{s} \le t_a \le 36.26\,\text{s}$. The aerodynamic parameters at the moment t_{a0} are introduced into (16) and (18). Among them, $I = 0.6$, $\alpha = 0.048$, $\sigma = 1.01$, and $\lambda = -0.0046$. It is assumed that $a = 10$ in (18), and $\Delta t_{\min} = 0.39$ s and $\Delta T_{\min} = 2.16$ s can be obtained through calculation. Then, based on (19), the constraint can be calculated to obtain the number of corrections n as $n < n_{\max} = 15.28 \approx 15$.

The swarm size in the PSO-CS algorithm is $N = 20$, and the acceleration factors are $c_1 = c_2 = 1.8$. The corresponding number of nests is 20, $\tau = 1.5$, $P_a = 0.25$, and the number of iterations is set to 100.

Using the calculation process in Section 4.2, the PSO algorithm is first used to calculate different small populations ($n_{\max} - 1 = 14$) under the same calculation conditions. It is assumed that the initial start control time t_0 is 19 s. The correction interval times are the same for each group and satisfy the inequality constraint. Set $k_1 = 0.7$ and $k_2 = 0.3$. The values of the proportional factors satisfy (28). Then, the minimum fitness of the objective function f_1 is calculated by Equation (27).

The calculation results for the different swarms are shown in Table 1. The population of the particle with the minimum fitness is $n_i = 7$, i.e., the optimal number of corrections of the projectile is 7. When $n_i = 13$ and 14, the required time is higher than the flight time. Therefore, it is not calculated.

Secondly, the PSO-CS algorithm is used to continue calculating the population of $n_i = 7$. The start control time is not set, and the optimal particle is searched in the full range. Set $k_2 = 0.3$ and $k_3 = 0.7$. The values of the proportional factors satisfy (30). Then, the minimum fitness of the objective function f_2 is calculated by Equation (29).

The curves in Figure 9 represent the changing trend of the fitness of the objective function in the iteration process when $n_i = 7$ population is calculated using the traditional PSO algorithm, the CS algorithm, and the PSO-CS algorithm. It can be seen that the minimum fitness values calculated by the PSO and CS algorithms are about 0.29 and 0.27, respectively. The minimum fitness calculated by the PSO-CS algorithm is 0.18. Table 2 compares the optimal results calculated by using three different algorithms.

Through comparison, it can be seen that the PSO algorithm calculation is easy to fall into local optimum, and the search ability in the later stage of iteration is poor. The

Table 1: Calculation results of different swarms.

Number of corrections	Fitness	ΔE (m)	Number of corrections	Fitness	ΔE (m)	Number of corrections	Fitness	ΔE (m)
3	2.29	71.92	7	0.46	5.24	11	0.60	3.48
4	1.66	49.25	8	0.51	5.15	12	0.65	3.67
5	1.12	29.75	9	0.53	4.34	13	——	——
6	0.67	13.52	10	0.57	4.19	14	——	——

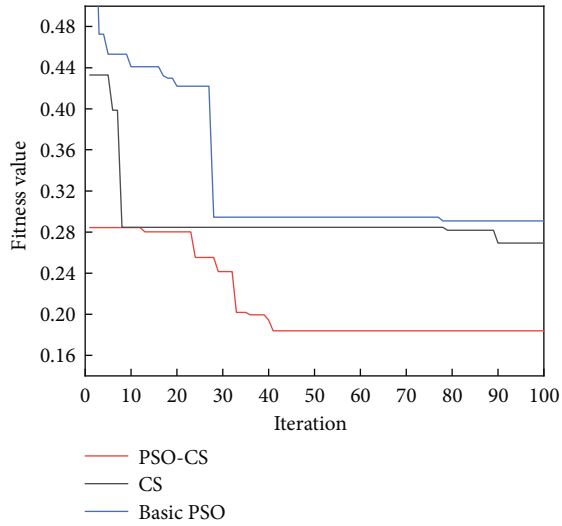

Figure 9: Comparison of the calculation results between PSO, CS, and PSO-CS algorithms.

Table 2: The optimal results calculated by three different algorithms.

$n_i = 7$	Optimal start control time t_a (s)	ΔE (m)	Fitness
PSO	21.15	3.49	0.29
CS	23.59	4.30	0.27
PSO-CS	24.58	5.03	0.18

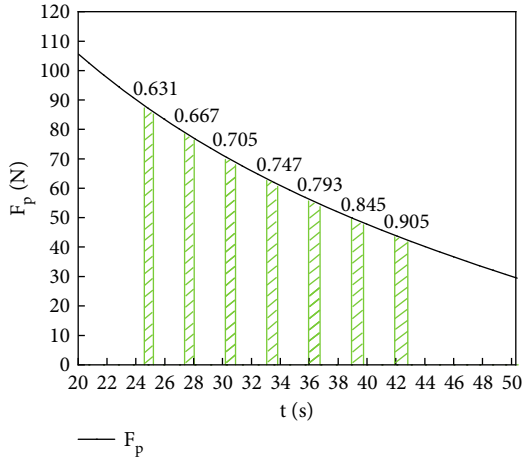

Figure 10: A schematic diagram of projectile optimal correction working parameters.

Table 3: The correction working parameters in the scheme.

Order number	Working time (s)	Interval time (s)	Order number	Working time (s)	Interval time (s)
1	0.631	2.160	5	0.793	2.163
2	0.667	2.164	6	0.845	2.162
3	0.705	2.162	7	0.905	——
4	0.747	2.162			

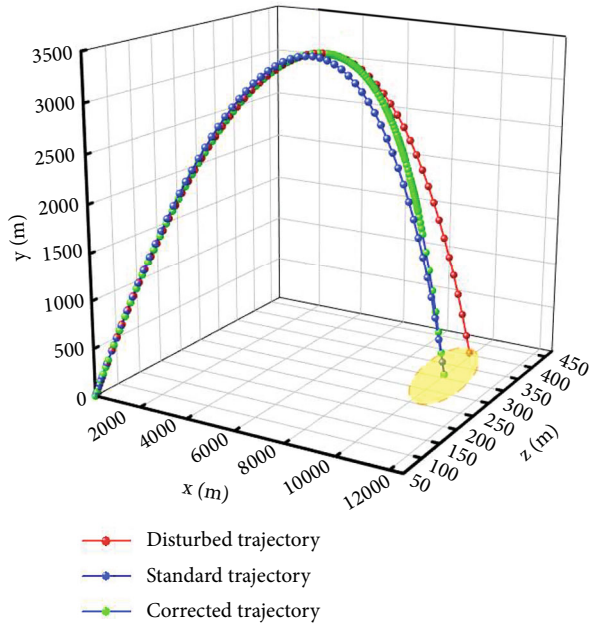

Figure 11: The trajectory curves of the projectile under three different conditions.

CS algorithm has strong global search ability, and it is not easy to fall into local optimum during calculation, but the convergence speed is slow. Under the same calculation conditions, the fitness calculated by PSO-CS algorithm is better, and the start control time is the latest. This is because the PSO-CS algorithm retains the advantages of their respective algorithms.

The PSO-CS algorithm first uses the PSO algorithm to update the particles of each generation and then substitutes the optimal particle position into the CS algorithm to continue updating. The particle is updated and calculated once by the CS algorithm based on the calculation of the PSO algorithm. This can guide the PSO and CS algorithms to quickly find the optimal solution, and the optimization ability of the single algorithm is improved. Therefore, the

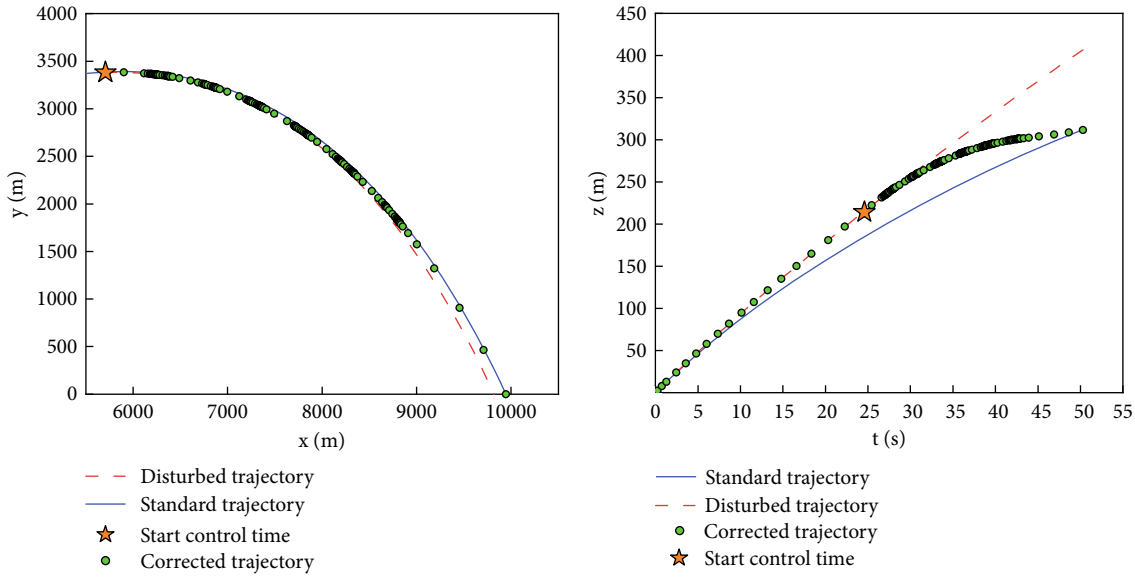

(a) Flight trajectory changing with time in the x-y direction

(b) Flight trajectory changing with time in the z direction

Figure 12: Comparison of trajectory curves in different directions.

accuracy of the PSO-CS hybrid algorithm is significantly better than their respective algorithms.

At the same time, the PSO-CS algorithm is superior to their respective algorithms in terms of iterative convergence speed. The fitness remains stable once the iteration time reaches 42, indicating that the particles have reached the optimal global position. The PSO-CS algorithm can effectively improve the search ability and accelerate the convergence speed of the algorithm.

Figure 10 represents a schematic diagram of the projectile's optimal correction working parameters calculated by the PSO-CS algorithm. The green area indicates the correction impulse. Since the correction force F_p is proportional to $v_{O\xi}$, the correction force decreases with an increase in the flight time. Since the limited allowable value $\Delta\delta_{\max}$ of the angle-of-attack increment is fixed, the single correction working time increases with a decrease in the correction force. At the same time, there is a certain interval time between the start control time $t_a = 24.58$ s calculated by the algorithm and the design start time $t_{a0} = 10.25$ s for the correction strategy, which is conducive to error accumulation. The specific parameter values of the working time and interval time of each correction action are shown in Table 3.

The flight trajectory curve of the projectile using this control strategy is simulated using the above calculated optimal correction working parameters combined with the flight motion equation, as shown in the green curve in Figure 11.

Figure 12 shows the comparison of the trajectory curve of the projectile in the x, y, and z directions under three different conditions. Compared with the standard flight trajectory, the impact point deviation of the disturbed projectile in the x direction is 127.62 m, the deviation in the z direction is 94.61 m, and the total deviation is 158.86 m. Under the correction action, the impact point deviation in the x direction is reduced to 4.23 m. The impact point deviation in the z direction is reduced to 2.72 m, and the total deviation from the target is less than 10 m, indicating that this control strategy can effectively correct the impact point deviation of the projectile.

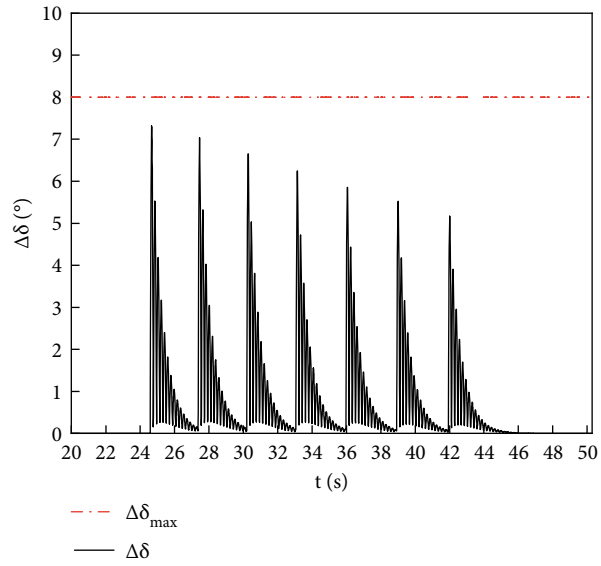

Figure 13: The variation curve of the amplitude of angle-of-attack increment with time.

The optimal correction working parameters calculated by the algorithm are used to simulate the amplitude curve of the flight angle-of-attack increment of the projectile caused by the correction action, as shown in Figure 13. The amplitude of the angle-of-attack increment is stable, and the maximum value does not exceed the set limited allowable value $\Delta\delta_{\max}$. Furthermore, the optimal correction work strategy can guide the projectile to correct the trajectory and make the projectile flight stable.

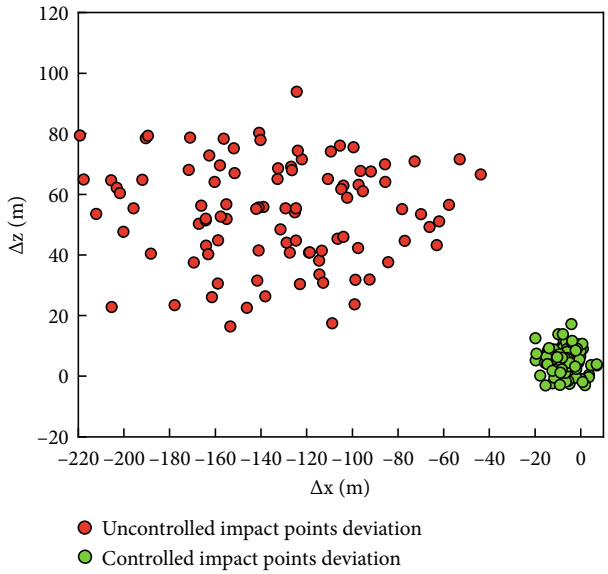

Figure 14: The impact point dispersion cases of the projectile in uncontrolled and controlled states.

Finally, the impact point dispersion cases of the projectile in the uncontrolled and controlled states are analyzed under the influence of different random disturbances. Random disturbance factors that cause the impact point dispersion of the projectile are mainly the interference brought by the launching process and wind influence. The disturbance of the launching process is reflected in the influence on the projectile's initial velocity. The above trajectory model is continued to be used and calculated. The relative error rate of the set initial velocity is 0.005, and the wind velocity is within the range of 5 m/s. Random disturbance factors all obey the normal distribution.

The impact point dispersion cases of the projectile in uncontrolled and controlled states are obtained by 100 Monte Carlo simulations, as shown in Figure 14. The air duct structure projectile is disturbed by the initial velocity error and wind velocity under uncontrolled conditions, and the impact point dispersion is large. The circular error probable (CEP) is obtained as 42.3 m, while the deviations between all uncontrolled impact points and the target are large. The impact point dispersion is significantly reduced when the projectile is corrected using this correction control strategy. The CEP under controlled conditions is 4.6 m, all controlled impact points have a small deviation from the target, and the impact point accuracy of the projectile is improved.

In this paper, the mathematical model of the projectile is established by analyzing the correction principle of the new air duct structure projectile. The effect of the correction action on the projectile is expressed in mathematical form. Then, based on the flight motion equation and dynamic equation of the projectile, the optimization method of projectile trajectory correction control strategy based on the PSO-CS hybrid algorithm is designed by using the multiobjective optimization method. The correction control strategy calculated in this way can effectively reduce the impact point deviation and impact point dispersion while making the projectile flight stable. And the projectile has a good correction effect.

6. Conclusions

In this paper, aiming at the trajectory correction control problem of a new air duct structure projectile, the control strategy of the correction mechanism was studied, and a design method of the optimal trajectory correction control strategy based on the PSO-CS hybrid algorithm was proposed. The contributions of this paper are summarized as follows:

(1) The mathematical model of the new air duct structure projectile was established by analyzing the correction principle. The correction control variables, such as the start control time, the number of corrections, the correction working time, and the interval time, were determined to establish the trajectory correction control strategy optimization model suitable for this type of projectile. Then, the control strategy optimization model's calculation method was designed using the PSO-CS hybrid algorithm

(2) The control strategy optimization model of the projectile was simulated and calculated using the PSO-CS hybrid algorithm. Then, the correction strategy in the current flight state was determined, and a set of optimal correction working parameters was obtained. Compared with the traditional PSO and CS algorithms, the PSO-CS hybrid algorithm is characterized by higher calculation accuracy, and the correction control strategy calculated via the PSO-CS hybrid algorithm is better. The trajectory curves of the projectile under three different conditions were simulated by solving the flight motion equation. Through comparison, it can be seen that the impact point deviation caused by a disturbance can be effectively reduced using the proposed control strategy to correct the projectile. The impact point deviation was reduced from 158.86 m to within 10 m

At the same time, the calculated start control time was later than the design start moment for the correction strategy, which accumulates errors, increases the correction range, and makes full use of the correction ability while ensuring the correction accuracy. The amplitude curve of the projectile flight angle-of-attack increment was simulated using the calculated correction working parameters. The amplitude of the angle-of-attack increment was stable, and the maximum value did not exceed the set limited allowable range. The control strategy can make the projectile flight stable.

(3) The Monte Carlo method was used to simulate dispersion cases of the projectile impact point in uncontrolled and controlled states. Compared with the impact point dispersion under uncontrolled conditions, the impact point dispersion after the

projectile was corrected by the proposed correction control strategy was significantly reduced. The CEP is reduced from 42.3 m to 4.6 m, and the impact point accuracy of the controlled projectile was improved. The validity of the optimization design method of control strategy proposed in this paper for trajectory correction of the projectile was verified by simulating the impact point case of the controlled projectile under different random disturbances for many times

In this paper, we used the step-by-step optimization method to calculate the projectile correction control strategy optimization model. When solving a function with multiple optimization goals, the optimal number of corrections was determined by setting the initial start control time and calculating the other optimization goals. Then, according to the determined optimal number of corrections, the optimal start control time was calculated. This calculation method has certain limitations. The setting of the initial start control time may have an impact on determining the optimal correction scheme.

In future research work, we will investigate the optimal design method for the initial start control time of the projectile under different flight conditions to reduce the impact on determining the optimal correction scheme. At the same time, in order to reduce the calculation time of the trajectory correction control strategy optimization model, we will improve the specific calculation method of the PSO-CS hybrid algorithm currently used.

Data Availability

The data used to support the findings of this study are available from the corresponding author upon request.

Conflicts of Interest

The authors declare no conflicts of interest.

Acknowledgments

This work was supported by the National Defense Pre-Research Foundation (Grant No. 61402060103).

References

[1] S. Theodoulis, V. Gassmann, P. Wernert, L. Dritsas, I. Kitsios, and A. Tzes, "Guidance and control design for a class of spin-stabilized fin-controlled projectiles," *Journal of Guidance, Control, and Dynamics*, vol. 36, no. 2, pp. 517–531, 2013.

[2] P. Wernert, "Stability analysis for canard guided dual-spin stabilized projectiles," in *AIAA Atmospheric Flight Mechanics Conference and Exhibit*, pp. 1–24, Chicago, Illinois, August 2009.

[3] Y. Wang, W. D. Song, D. Fang, and Q. W. Guo, "Guidance and control design for a class of spin-stabilized projectiles with a two-dimensional trajectory correction fuze," *International Journal of Aerospace Engineering*, vol. 2015, Article ID 908304, 15 pages, 2015.

[4] J. Guan and W. J. Yi, "Modeling of dual-spinning projectile with canard and trajectory filtering," *International Journal of Aerospace Engineering*, vol. 2018, Article ID 1795158, 7 pages, 2018.

[5] Y. Wang, X. M. Wang, and J. Y. Yu, "Influence of control strategy on stability of dual-spin projectiles with fixed canards," *Defence Technology*, vol. 14, no. 6, pp. 709–719, 2018.

[6] R. P. Li, D. G. Li, and J. R. Fan, "Dynamic response analysis for a terminal guided projectile with a trajectory correction fuze," *IEEE Access*, vol. 7, pp. 94994–95007, 2019.

[7] Q. S. Zheng and Z. M. Zhou, "Flight stability of canard-guided dual-spin projectiles with angular rate loops," *International Journal of Aerospace Engineering*, vol. 2020, Article ID 2705175, 9 pages, 2020.

[8] S. Chandgadkar, M. Costello, B. Dano, J. Liburdy, and D. Pence, "Performance of a smart direct fire projectile using a ram air control mechanism," *Journal of Dynamic Systems, Measurement, and Control*, vol. 124, no. 4, pp. 606–612, 2002.

[9] S. L. Cui, X. Liu, S. S. Jiang, and J. C. Guo, "Control strategies for flight stability of trajectory correction projectile with air-ducts structure," *Mathematical Problems in Engineering*, vol. 2022, Article ID 1383294, 16 pages, 2022.

[10] S. L. Cui, X. Liu, S. S. Jiang, and J. C. Guo, "Research on aerodynamic characteristics of a spin-stabilized projectile with air-ducts structure," *Mechanical Science and Technology for Aerospace Engineering*, vol. 41, no. 7, pp. 1136–1141, 2022.

[11] B. Burchett and M. Costello, "Model predictive lateral pulse jet control of an atmospheric rocket," *Journal of Guidance, Control, and Dynamics*, vol. 25, no. 5, pp. 860–867, 2002.

[12] Y. J. Cao, S. X. Yang, and X. J. Li, "Research on firing phase angle optimization of terminal trajectory correction projectile based on pulse jet control," *Acta Armamentarii*, vol. 29, no. 8, pp. 897–901, 2008.

[13] M. Gao, Y. W. Zhang, and S. C. Yang, "Firing control optimization of impulse thrusters for trajectory correction projectiles," *International Journal of Aerospace Engineering*, vol. 2015, Article ID 781472, 11 pages, 2015.

[14] B. Burchett, "Genetic algorithm optimization of hydra pulse jet controller," in *AIAA Atmospheric Flight Mechanics Conference and Exhibit*, pp. 1–13, Honolulu, Hawaii, August 2008.

[15] H. Gui, R. S. Sun, W. Chen, and B. Zhu, "Reaction control system optimization for maneuverable reentry vehicles based on particle swarm optimization," *Discrete Dynamics in Nature and Society*, vol. 2020, Article ID 6518531, 11 pages, 2020.

[16] J. Kennedy and R. Eberhart, "Particle swarm optimization," in *Proceedings of ICNN'95- International Conference on Neural Networks*, Perth, Australia, November 1995.

[17] M. Zhang, X. Chen, and Y. P. Lu, "Optimization of performance weighted function for missile robust controller using PSO algorithm," *Journal of Applied Sciences*, vol. 29, no. 6, pp. 650–654, 2011.

[18] X. F. Song, Y. Zhang, D. W. Gong, and X. Z. Gao, "A fast hybrid feature selection based on correlation-guided clustering and particle swarm optimization for high-dimensional data," *IEEE Transactions on Cybernetics*, vol. 52, no. 9, pp. 9573–9586, 2022.

[19] X. F. Ji, Y. Zhang, D. W. Gong, X. Y. Sun, and Y. N. Guo, "Multisurrogate-assisted multitasking particle swarm optimization for expensive multimodal problems," *IEEE Transactions on Cybernetics*, vol. 53, no. 4, pp. 2516–2530, 2021.

[20] H. W. Yang, L. H. Dou, and M. G. Gan, "A particle swarm optimization for fuel-optimal impulsive control problems of guided projectile," in *2010 Chinese Control and Decision Conference*, pp. 3034–3038, Xuzhou, China, May 2010.

[21] R. S. Sun, Q. Hong, and G. Zhu, "A novel optimal control method for impulsive-correction projectile based on particle swarm optimization," *Discrete Dynamics in Nature and Society*, vol. 2016, Article ID 5098784, 9 pages, 2016.

[22] Z. Yang, J. Fu, L. M. Wang, and Z. Chen, "Intelligent optimal pulse-jet control for dual-spin projectiles," in *Proceedings of the 40th Chinese Control Conference*, pp. 7639–7644, Shanghai, China, July 2021.

[23] P. J. Angeline, "Evolutionary optimization versus particle swarm optimization: philosophy and performance differences," in *International Conference on Evolutionary Programming*, pp. 601–610, Springer, 1998.

[24] K. E. Parsopoulos and M. N. Vrahatis, *Particle Swarm Optimization and Intelligence: Advances and Applications*, Information Science Reference, New York, USA, Hershey, PA, 2010.

[25] B. H. Abed-alguni, "Island-based cuckoo search with highly disruptive polynomial mutation," *International Journal of Artificial Intelligence*, vol. 17, no. 1, pp. 57–82, 2019.

[26] B. H. Abed-alguni and D. J. Paul, "Hybridizing the cuckoo search algorithm with different mutation operators for numerical optimization problems," *Journal of Intelligent Systems*, vol. 29, no. 1, pp. 1043–1062, 2020.

[27] B. H. Abed-alguni, N. A. Alawad, M. Barhoush, and R. Hammad, "Exploratory cuckoo search for solving single-objective optimization problems," *Soft Computing*, vol. 25, no. 15, pp. 10167–10180, 2021.

[28] F. Alkhateeb, B. H. Abed-alguni, and M. H. Al-rousan, "Discrete hybrid cuckoo search and simulated annealing algorithm for solving the job shop scheduling problem," *The Journal of Supercomputing*, vol. 78, no. 4, pp. 4799–4826, 2022.

[29] F. Wang, L. G. Luo, X. S. He, and Y. Wang, "Hybrid optimization algorithm of PSO and cuckoo search," in *2nd International Conference on Artificial Intelligence, Management Science and Electronic Commerce*, pp. 1172–1175, Dengleng, August 2011.

[30] M. Karthikeyan and K. Venkatalakshmi, "Energy conscious clustering of wireless sensor network using PSO incorporated cuckoo search," in *2012 Third International Conference on Computing, Communication and Networking Technologies*, pp. 1–7, Coimbatore, India, July 2012.

[31] B. M. Feng and W. S. Nie, "A new method for initial parameters optimization of guided projectiles," *International Journal of Aerospace Engineering*, vol. 2013, Article ID 486020, 7 pages, 2013.

[32] Y. W. Zhang, M. Gao, S. C. Yang, and D. Fang, "Optimization of trajectory correction scheme for guided mortar projectiles," *International Journal of Aerospace Engineering*, vol. 2015, Article ID 618458, 14 pages, 2015.

[33] Z. P. Han, *Exterior Ballistics of Projectiles and Rockets*, Beijing Institute of Technology Press, Beijing, China, 2014.

[34] F. Sève, S. Theodoulis, P. Wernert, M. Zasadzinski, and M. Boutayeb, "Flight dynamics modeling of dual-spin guided projectiles," *IEEE Transactions on Aerospace and Electronic Systems*, vol. 53, no. 4, pp. 1625–1641, 2017.

[35] A. Calise and H. El-Shirbiny, "An analysis of aerodynamic control for direct fire spinning projectiles," in *AIAA Guidance, Navigation, and Control Conference and Exhibit*, pp. 1–10, Montreal, Canada, August 2001.

[36] X. S. Yang and S. Deb, "Cuckoo search via Lévy flights," in *2009 World Congress on Nature & Biologically Inspired Computing*, pp. 210–214, Coimbatore, India, December 2009.

[37] X. S. Yang and S. Deb, "Engineering optimisation by cuckoo search," *International Journal of Mathematical Modelling and Numerical Optimisation*, vol. 1, no. 4, pp. 330–343, 2010.

[38] C. Y. Dong, Y. Lu, W. L. Jiang, and Q. Wang, "Fault tolerant control based on cuckoo search algorithm for a class of morphing aircraft," *Acta Aeronautica et Astronautica Sinica*, vol. 36, no. 6, pp. 2047–2054, 2015.